

DIAMOND WINGS IN SUPERSONIC FLOW WITH SLIP

F.A. Maksimov^{1,2}, N.A. Ostapenko¹, M.A. Zubin¹¹Institute of Mechanics, Lomonosov Moscow State University, Moscow, ostap@imec.msu.ru²Institute of Computer Aided Design, Russian Academy of Sciences, Moscow, f_a_maximov@mail.ru

Abstract. The results of numerical and experimental studies of asymmetric flow around diamond wings on modes with attached shock waves or centered rarefaction waves on the leading edges with the Mach number $M=3$ are presented.

The computation codes of second-order approximation were developed on special grids within the ideal gas model, which made it possible to obtain original data on asymmetric flow around diamond wings. A wide variety of flow patterns in the shock layer was found, depending on the Mach number, angles of attack and slip, due to presence of the breakpoint of the transverse wing outline. In particular, disruption of flow from the windward console and presence of a vortex on the flow modes with slip and subsonic (transverse) flow in the vicinity of the central chord of the wing; the existence of trans- and supersonic flow along the vortex circumference and in the return flow near the wall of the lee console with the formation of shock waves with increasing slip angle were found. Approaching of the spreading point of streamlines, closing the vortex, and the node of streamlines on the lee console surface are typical for one of the sequences of flow patterns, occurring at the moderate Mach numbers of the undisturbed flow with increasing slip angle. When an outline of conditions is realized in the vicinity of the breakpoint that allow for the existence of a centered rarefaction wave, the vortex moves downstream along the wing surface, and a shock wave forms in front of it. After ‘merging’ of the indicated spreading point and node of streamlines on the leeward console, only the flowing down point remains, which includes streamlines from the front edges of the wing and Ferry vortex singularity above it.

The existence of flow patterns with the formation of a vortex on the lee outer wing in the vicinity of the central chord was confirmed in the experiments with $M=3$ using various methods, in particular, a special shadow method for visualizing conical flows.

The results of a numerical study of the possibility of controlling the flow structure near a diamond wing with slip are presented. A half-angle of a circular cone solution, inscribed in the inner dihedral angle between the flat wing consoles, was used as a control parameter to eliminate its fracture along the central chord. It is shown that such a control method is an effective means for eliminating vortex structures on the lee outer wing, when it is being flowed around with slip, that generate critical lines on the surface in a conical flow with intensive flow spreading around which high heat flows can occur in a real flow. The classification of vortex structures in the shock layer in the presence of rounding in the vicinity of the plane of symmetry of the wing is carried out. Criteria for the existence of Ferry vortex singularities in the absence of branching points of shock waves are determined.

1. The calculation method. A computational code of the second order of approximation was developed to study flow around the wings of the diamond geometry (Fig. 1a; x, y, z - Cartesian coordinate system; β, γ - the angle at the top of the consoles and opening angle of the wing; U_∞ - the rate of the undisturbed flow; α, ϑ - the angles of attack and slip) with the attached shock waves or centered rarefaction waves at the leading edges within the ideal gas model.

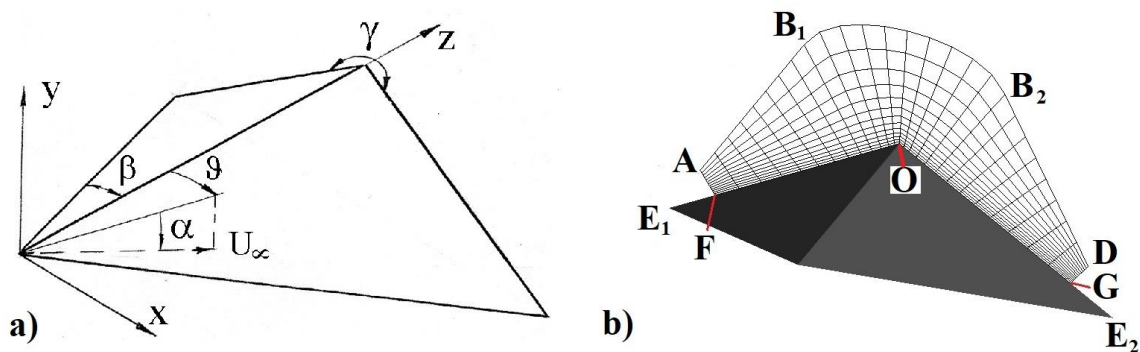


Figure 1. Diamond wing (a) and computational grid (b).

Figure 1b shows an example of a calculation grid. The FOG boundary is located on the surface of the wing, the AB_1B_2D one is in the undisturbed flow. The intersection point of lines OF and AB_1 corresponds to right edge E_1 . Similarly, straight lines OG and DB_2 intersect at left edge of E_2 . The condition of flow conicity is set (the condition

that the derivative of the gas-dynamic functions are zero along the rays from the wing edges) relative to edges E_1 and E_2 at boundaries AF and DG. Boundaries AF and DG should be in the area that is not influenced by the central part of the wing. The conditions are set in the incident flow at boundary AB_1B_2D , and the condition of no-flow - at boundaries FO and OG. The distribution of nodes is determined by a parabolic generator in the computational domain - the grid is constructed by layers from the body, normal to the surface of the body at the beginning and then towards the nodes, specified on the outer boundary. The nodes of the computational grid thickened towards the edge and along the normal to the surface of the wing.

The method of numerical simulation is given in [1-3]. An effective way to speed up establishment is to use a local integration step when calculating on non-uniform grids.

2. Flow structure near diamond wings. Below are some data on the flow structure in the shock layer near the wing with a console angle $\beta=45^\circ$, an opening angle $\gamma=240^\circ$, obtained as a result of numerical calculations of flow within the Euler model with $M=3$, $\alpha=4^\circ$, at different values of slip angle ϑ .

Let us turn to the modes when flowing over begins from the windward console to the leeward one (from the left console to the right one in the figures below) in accordance with the choice of direction of increasing slip angle ϑ . There can be no breaks in streamlines during the transition of the central chord of the wing in subsonic (transverse) flow. Therefore, one should expect flow separation when it leaves the windward console and, most likely, a vortex is formed, that is, a streamline appears, which is a part of a spreading point on the lee console, to the left of which there are many streamlines, forming a vortex, and there is set of streamlines, forming the structure of flow outside the vortex, to the right. This happens with an increase in the slip angle in a certain neighborhood of zero, where the resolution of the grid allows one to observe the specified vortex, the size of which grows with the increasing slip angle. Figure 2a, b shows pressure isolines in the entire area of the disturbed flow and streamlines of the transverse flow against the background of the density distribution in the central chord of the wing at $\alpha=4^\circ$, $\vartheta=5^\circ$. The vortex region is highlighted in white in Figure 2a, in which pressure is less than 1.

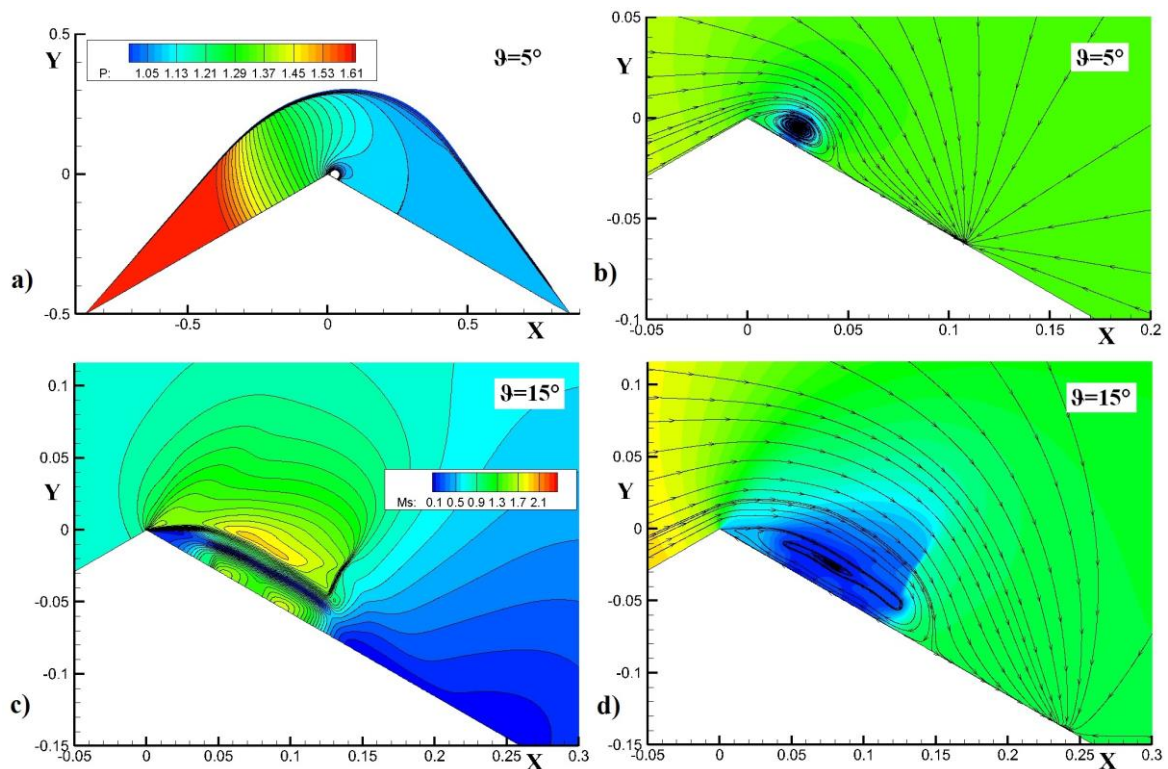


Figure 2. Flow near wing ($\beta=45^\circ$, $\gamma=240^\circ$) with $M=3$, $\alpha=4^\circ$ and various values of ϑ .

a, b - isolines of pressure and streamlines at $\vartheta=5^\circ$.

c, d - isolines of transverse Mach number and streamlines at $\vartheta=15^\circ$.

With a further increase in the slip angle along the vortex bypass, the transonic flow is formed, in which the supersonic area is closed by a compression shock. An example of such flow is shown in Fig. 2c, d by a fragment in the vicinity of the breaking point of the transverse wing outline at $\vartheta=15^\circ$, where the isomachs of the transverse conical flow and streamlines (lines with arrows) are shown against the background of density distribution. In addition to the above-mentioned cross-flow properties, the nearly wedge-shaped vortex in the breaking point vicinity attracts attention. The streamlined outline, consisting of a segment of the outline of the windward outer wing and a liquid 'wedge', suffers a fracture, but smaller than the wing outline. This indicates the formation of a centered rarefaction wave at the breaking point. It is observed among the isomachs. The transonic nature of the return flow in a vortex in the vicinity of the wall should also be attributed to the unexpected properties of flow.

Figure 3 shows distances $L = \text{tg}(\varphi)$ (φ is the angle between the central chord of the wing and beam of the conical coordinate system passing through the critical point) from the central chord to various types of critical points in interval $[1^\circ, 25^\circ]$ of the slip angle change. Points 1 correspond to the position of the flowing down points on the lee outer wing, points 2 - to the position of the spreading point. Dots 3 indicate the beginning of a vortex. When the corresponding $L=0$ ($\vartheta < 18^\circ$), a vortex occurs when flow breaks off from the corner point of the transverse outline. When $L>0$, the beginning of a vortex (flowing down point) moves from the corner point downstream. There is a centered rarefaction wave for flow on a sphere at the corner point. A shock wave is formed in front of the vortex, and the supersonic area above the vortex is closed by a compression shock. The shock-wave structure, accompanying the vortex on the lee outer wing in the considered flow condition, can be called the λ -configuration of shock waves.

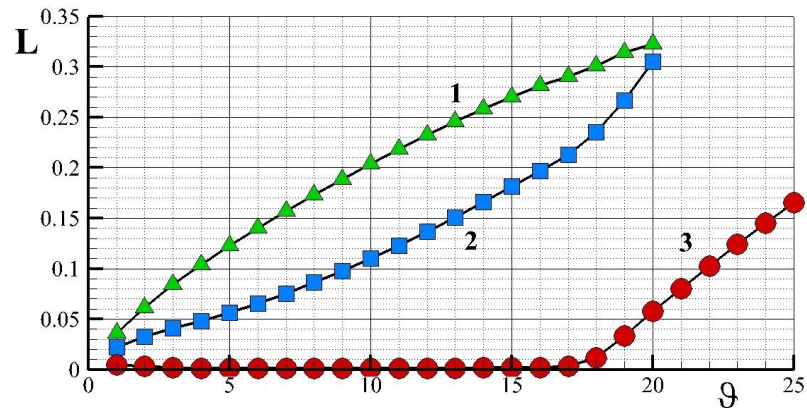


Figure 3. Position of critical points on the lee outer wing:
1 - node of streamlines; 2 - spreading point; 3 - beginning of vortex or flowing down point.

According to calculations (Fig. 3) there is also a streamline node (point 1) behind the point of the vortex attachment (spreading point 2) with $\leq 20^\circ$. This condition is shown in Fig. 4a, b at $\vartheta=19^\circ$, where the isolines of the transverse Mach number of conical flow on the sphere and streamlines against the background of the density distribution are shown.

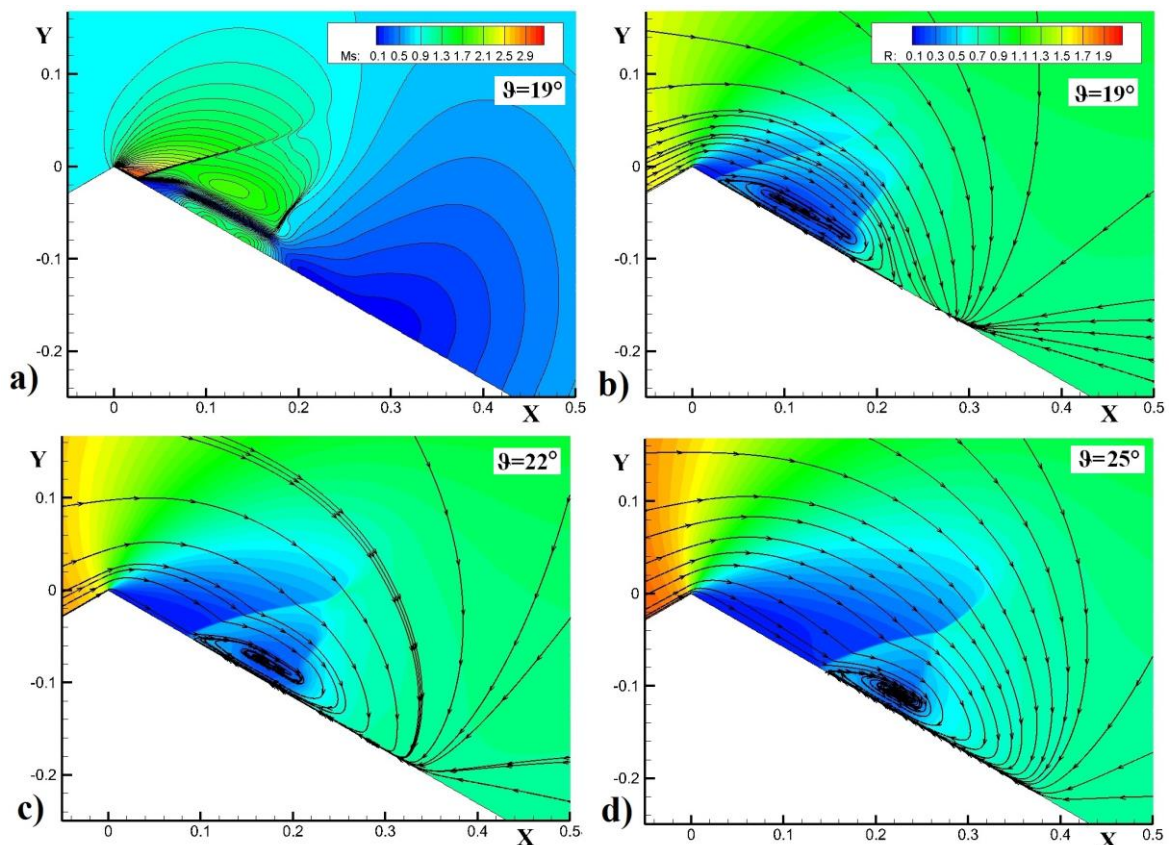


Figure 4. Flow near wing ($\beta=45^\circ$, $\gamma=240^\circ$) with $M=3$, $\alpha=4^\circ$ and various values of ϑ .
a, b - isolines of transverse Mach number and streamlines at $\vartheta=19^\circ$.
c, d - streamlines at $\vartheta=22$ and 25° .

At $\vartheta \approx 20 \div 21^\circ$, the streamline node and point of the vortex attachment (point 2) 'merge' and with increasing ϑ the only critical point of the saddle type remains on the lee outer wing - the flowing down point (Fig. 3), corresponding to the beginning of a vortex (point 3) at $\vartheta < 21^\circ$. All streamlines enter a single singular point in such flow conditions - the Ferry vortex singularity, which is located above the critical flowing down point on the surface of the leeward outer wing. This condition is presented in Fig. 4c, d, where streamlines are shown against the background of the density distribution at $\vartheta = 22$ and 25° .

One of the possible sequences of flow patterns around the wing, which occur at moderate Mach numbers of the undisturbed flow with increasing slip angle, is described here [4].

3. The experimental test. To test the existence of the above features of the flow structure on the lee outer wing in the vicinity of the central chord of the wing, found within the ideal gas theory, experimental studies of flow around a V-shaped wing with an opening angle $\gamma = 240^\circ$ and a corner at the top of the outer wing $\beta = 45^\circ$ when the number $M = 3$ were carried out [5, 6]. The following experimental techniques were used: optical visualization of flow in the plane normal to the central wing chord [7], pressure measurement on the outer wing surface and visualization of limiting streamlines. The drainage holes were located on the outer wing along its span in two sections $z = 63$ and 65 mm, in a staggered order with an angular distance between their centers of $\approx 2^\circ$. The single Reynolds number in the A-3 aerodynamic setup of the Institute of Mechanics, Lomonosov Moscow State University was 1.6×10^8 1/m, which ensured the completion of transition from laminar to a turbulent boundary layer at a distance of 10-15 mm from the top of the wing, the length of the central chord of which was 90 mm.

Figure 5 shows the experimental results and their comparison with the calculation under the conditions $\alpha = 4^\circ$, $\vartheta = 10^\circ$. Flow separation from the corner point of the transverse wing outline and two critical points on the lee outer wing take place under these conditions within the Euler equations. One point corresponds to the attachment of a detached flow, the second one - to the line of flowing down of current surfaces that did not fall into the vortex of a separated flow.

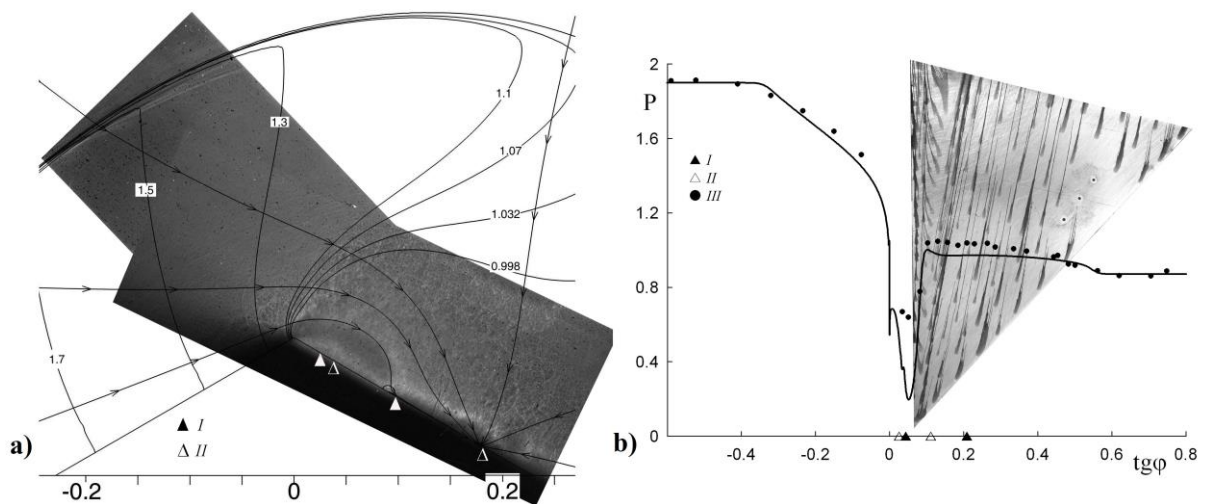


Figure 5. Experiment: symbols I and II position of flowing down and spreading lines; symbols III - experimental pressure values.

Figure 5a shows the arrangement with the results of numerical calculation of the pressure distribution in the shock layer, referred to pressure in the undisturbed flow (isobars are digitized solid lines), and images of flow in the transverse plane, obtained at two positions of the photo screen [7]. One can see a section of the head shock wave in the left image, the position of which is in good agreement with the calculated shape of the shock wave (concentration of isobars). There is a vortex, formed by a stream that has separated from a corner point, in the right image, the size and shape of which agree satisfactorily with streamline, closing the vortex area on the lee outer wing or, in other words, entering the spreading point obtained by numerical calculation. Symbols I and II indicate positions of the critical lines of the conic flow observed on the surface of the lee outer wing: flowing down and spreading, respectively, taken from the picture of the limiting streamlines shown in Fig. 5b.

Figure 5b shows pressure distribution P , referred to pressure in the undisturbed flow, on the wing surface on both sides from the breaking point of transverse wing outline depending on the tangent of angle φ between the central chord and considered point on the wing surface. Symbols I and II correspond to those in Fig. 5b, symbols III mark the experimental pressure values, the solid curve shows the calculated distribution R . The same figure shows the limit streamlines on the lee outer wing. As can be seen, the positions of the vortex attachment point in calculation (maximum on distribution curve P) and in the experiment (second left symbol II, in accordance with the pattern of limit streamlines) agree very well. Only pressure levels in the vortex area are different.

There is separation of the boundary layer, marked by the left pair of symbols I and II in Fig. 5a and Fig. 5b, in the experiment inside the vortex in the return subsonic flow in accordance with the pattern of limit streamlines (Fig. 5). This separation is not described within the Euler model [8], and this is precisely the reason for the rather noticeable mismatch P in the vortex area between calculation and the experiment.

4. Control of the Structure of Flow. The presence of vortex structures near the diamond wing in a fairly wide range of variation of the slip angle indicates the possibility of high heat flows to the outer wing in the vicinity of the closure point of the separated vortex — the points of flow attachment and spreading. This circumstance indicates that unfavorable conditions of heat transfer, generated by gas-dynamic structure of flow, can be realized in flow beyond the breaking point. This section presents some results of numerical study of the possibility to control the flow structure near the diamond wing [9]. Angle δ of a half opening of a circular cone, inscribed in the inner dihedral angle between the flat outer wings, is used as a control parameter to eliminate breaking of its surface along the central chord.

The method of numerical calculation used in the work is rather simply adapted to the geometry of a diamond wing with a conical rounding in the vicinity of the central chord. Angles of attack and slip are determined by the position of the central chord of the original wing without rounding. Pressure distribution on the wing surface in a conical flow is given depending on length of arc L of the cross section measured from the plane of symmetry of the wing.

The results of flow calculation around a diamond wing with angles $\gamma=240^\circ$ and $\beta=45^\circ$ with the Mach number of the undisturbed flow $M=3$ and 6 are presented within the ideal gas theory. The illustrative material refers to flow around the wing at $M=3$, $\alpha=4^\circ$, $\vartheta=10^\circ$ and various values of angle δ . Figure 6 shows the flow patterns on the lee outer wing in the vicinity of the plane of symmetry of the wings with $\delta=0^\circ$ (a) and $\delta=1^\circ$ (b) (isomachs on the sphere and streamlines are lines with arrows). A separated vortex with supersonic flow areas in the return flow and along its outer contour is realized behind the break point of the transverse outer wing at $\delta=0^\circ$. The flow structure at $\delta=1^\circ$ (Fig.6b) is qualitatively different from that one at $\delta=0^\circ$ (Fig.6a) in the vicinity of the plane of symmetry. Flow is accelerated to supersonic speeds on the sphere in the vicinity of rounding of the transverse outer wing, and a shock wave, normally falling on the wall, is formed with a velocity corresponding to the Mach number of flow speed at its base $Mn \approx 2.2$.

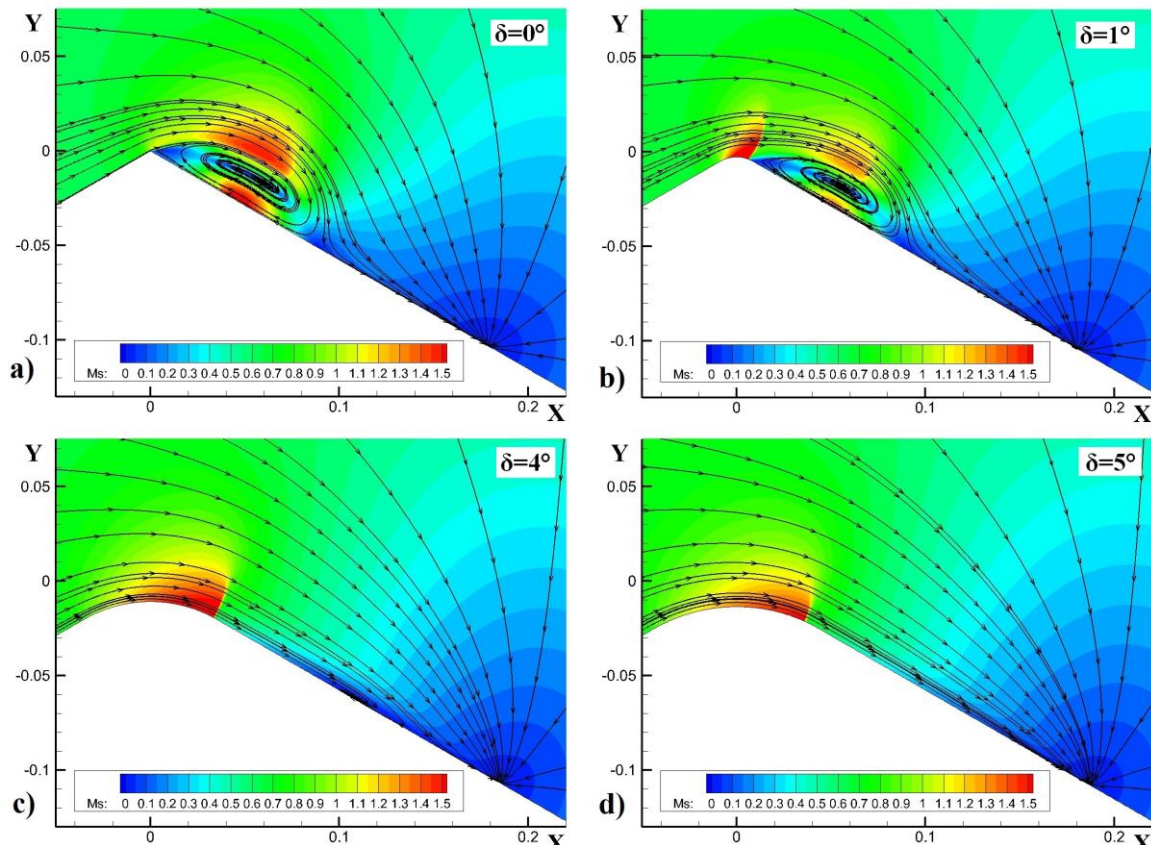


Figure 6. Flow near wing ($\beta=45^\circ$, $\gamma=240^\circ$) with $M=3$, $\alpha=4^\circ$, $\vartheta=10^\circ$.
a - $\delta=0^\circ$, b - $\delta=1^\circ$, c - $\delta=4^\circ$, d - $\delta=5^\circ$.

Dependence $Mn(\delta)$ is shown in Fig.7a. It follows that the shock wave, preceding the structure of critical points on the lee outer wing, will not cause separation of the turbulent boundary layer [3] at $\delta \approx 6^\circ$. Fig. 7b shows data on the location of critical points and other objects on lee outer wing L relative to the plane of symmetry of the wing, depending on δ . Symbols 1–3 respectively denote the front (flowing down) and rear (spreading) critical points

of the vortex, as well as the streamline node located downstream of the vortex. Symbols 4 and 5 mark the positions of the shock wave and conjugation point of the cone with half-angle of opening δ . The calculated points, denoted by symbols 1-5, are approximated by polynomials of various degrees (solid curves). The nonmonotonic dependence of the shock wave position from δ (symbols 4), as well as its practical coincidence with the conjugation point of the cone surface and the flat lee outer wing to $\delta \approx 4.7^\circ$, draw attention. The vortex, bounded by symbols 1-2, ceases to occur at $\delta \approx 4.5^\circ$. A streamline node (symbols 3) and a shock wave (symbols 4) continue to exist on the lee outer wing, providing retarding of the transverse flow from supersonic speeds to zero at the streamline node.

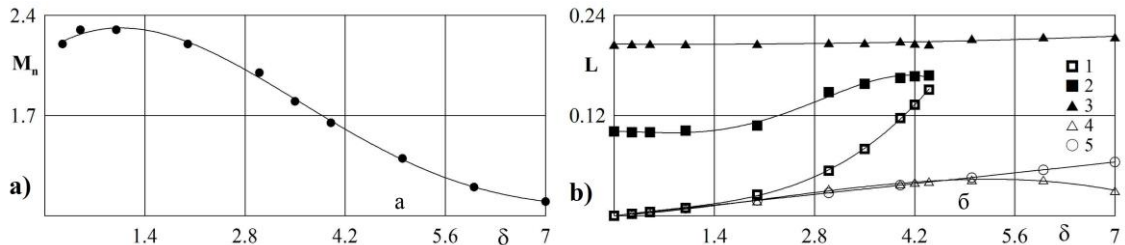


Figure 7. a) M_n - Mach number of velocity normal to incident shock wave on wall;
b) L - position on outer wing: 1,2 - front and rear critical points of vortex, 3 - node of streamlines, 4 - shock wave, 5 - conjugation point of outer wing and cone with half-angle δ .

Figure 8 shows pressure distributions related to pressure in the undisturbed flow on the surface of the wing, depending on length of arc L of the transverse outer wing, measured from its plane of symmetry. Curves 1–8 correspond to $\delta \in [0, 7]$ with step 1° . One should remember there is flow in both directions from maximum P ($L \approx 0.1$) when $\delta = 0$: to the left in the return vortex flow to the plane of symmetry with successive formation of two compression shocks and to the right up to the flowing down point of transverse flow (the node of streamlines at $L \approx 0.205$, Fig. 6a, 7b), whereas flow from the plane of symmetry of the wing is realized for $\delta > 0$ with formation of a shock wave. The critical points occur (symbols 1, 2) in interval $\delta \in (0, 4.5)$ downstream between the shock wave (Fig. 7b, symbols 4) and streamline node (symbols 3), and transverse flow takes place from the plane of symmetry of the wing to the streamline node for $\delta > 4.5^\circ$.

In general, it can be concluded that for the above values of the key parameters, rounding of the corner point of the transverse outline of a diamond wing provides such characteristics of the flow structure in the shock layer already for $\delta > 6^\circ$, for which both the critical spreading points and shock waves with intensity, sufficient to form a separation of a turbulent boundary layer in a real flow, are absent.

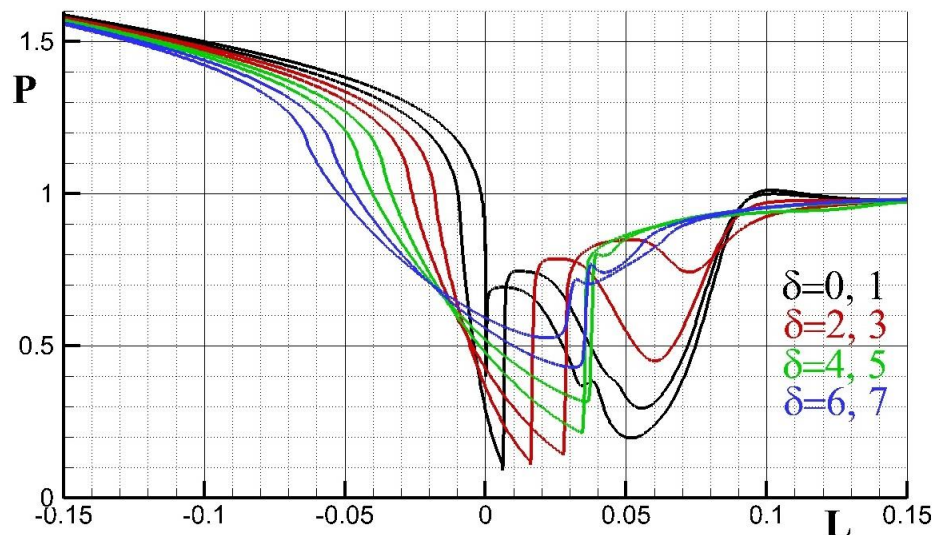


Figure 8. Pressure distribution on wing surface ($\beta = 45^\circ$, $\gamma = 240^\circ$) with $M = 3$, $\alpha = 4^\circ$, $\theta = 10^\circ$.
 $\delta = 0, 1, 2, 3, 4, 5, 6$ and 7° .

5. On criteria for existence of Ferry vortex singularities. Fig. 9a, b show flow patterns on the lee outer wing with $\delta = 3$ and 4° with entropy distribution and streamlines (lines with arrows). Similar sets of critical points were observed when flow around V-shaped wings in the plane of symmetry of flow [2] took place. The only difference is that the streamline node was located at the breaking point of the V-shaped wing outline. Two criteria were defined in [1], the fulfillment of which is necessary for the existence of the Ferry vortex singularities. This is Mach number M_n of velocity, normal to the beam passing through the branch point of the Mach configuration of shock waves, and total pressure jump ΔK at the corresponding contact discontinuity. As can be seen, the existence of branching points of shock waves is necessary for the existence of non-viscous vortex structures. However,

according to Figure 9, there are none. This fact allows us to conclude that presence of a contact discontinuity is not a mandatory requirement for the existence of the Ferry vortex singularity. In other words, the contact discontinuity can be represented by a gradient flow with a corresponding jump between the levels of total pressure (entropy) at its boundaries. The value of the Mach number of velocity, normal to the compression shock, the shape of which provides a gradient flow, should also be sufficient. If we accept this concept, then all the flow patterns observed in calculations receive a natural explanation.

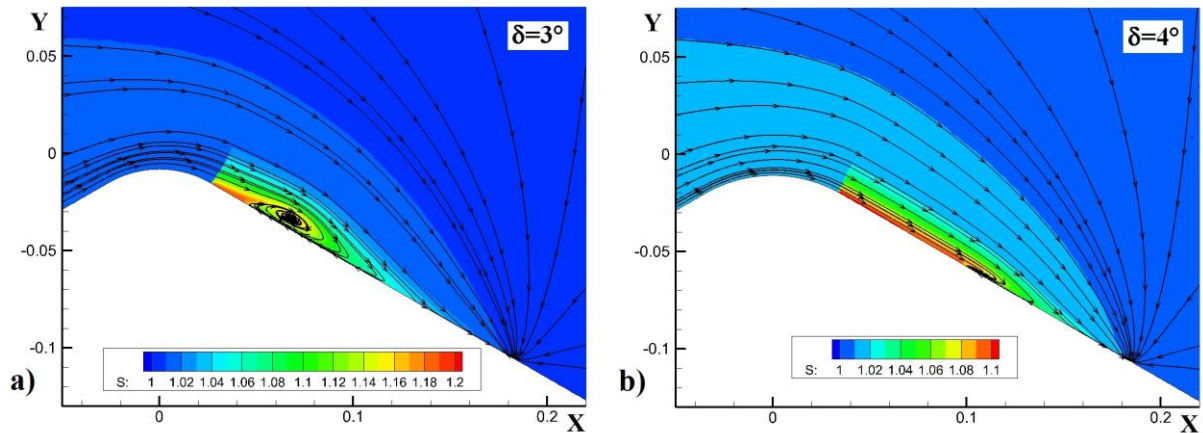


Figure 9. Flow near wing ($\gamma=240^\circ$, $\beta=45^\circ$) with $M=3$, $\alpha=4^\circ$, $\vartheta=10^\circ$ with entropy distribution and streamlines; a- $\delta=3^\circ$, b- $\delta=4^\circ$.

Figure 10a shows distributions of entropy function S along normal h to the wing surface ($\gamma=240^\circ$, $\beta=45^\circ$, $\alpha=4^\circ$, $\vartheta=10^\circ$, $M=3$) behind the shock wave formed before the vortex structure (curves 1–7 correspond to $\delta=0.25, 0.5, 1, 2, 3, 4, 5^\circ$).

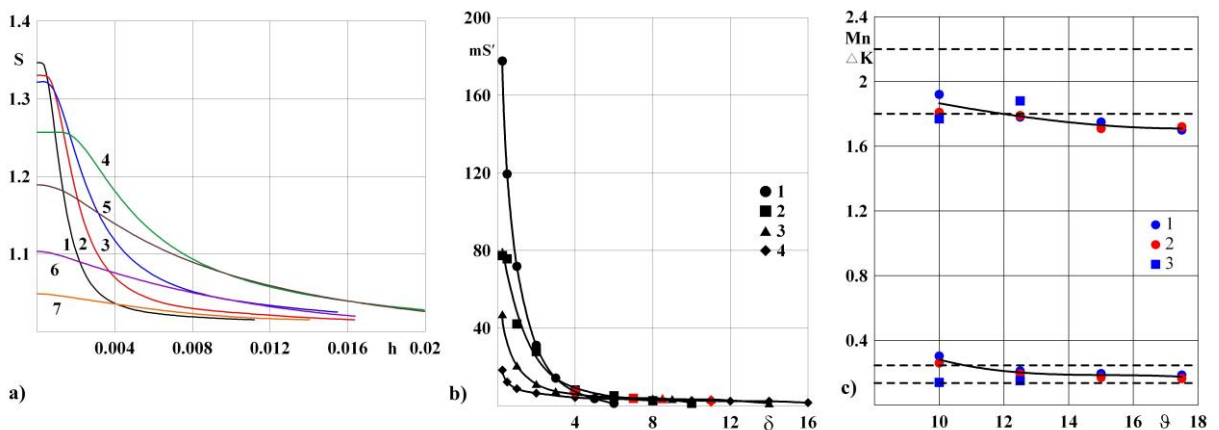


Figure 10. Distributions S behind shock wave - (a), mS' - (b).

Correlation of criterion values Mn and ΔK [1] (areas bounded by pairs of dashed straight lines) with their values determined by mS'^* and ΔS for changing type of flow - (c).

Identifying the position of an imaginary contact discontinuity, as mentioned above, with maximum derivative $\max S' = mS'$ with respect to h , we can conclude that mS' with increasing δ decreases, which corresponds to a decrease in the difference between maximum value S (on the wall) and its value at the periphery, and is a monotone function δ . The latter allows S' itself to be taken as a parameter characterizing the intensity of an imaginary contact discontinuity. Figure 10b presents dependences mS' for $M=3$, $\alpha=4^\circ$ and $\vartheta=10, 12.5, 15, 17.5$ (symbols 1–4).

The red symbols indicate values $mS' = mS'^*$, corresponding to disappearance of the Ferry vortex singularities in the flow structure. The proximity of ordinates of these points indicates the existence of a criterion for mS'^* , corresponding to transition from the flow structure containing the Ferry vortex singularity to structure without it. Analysis of the calculation results for $\alpha=10^\circ$ and $M=6$ allows us to draw a similar conclusion.

Figure 10c shows areas bounded by pairs of dashed straight lines, in which, according to [1], the criterial values of Mn and ΔK are located at $M=3$ and 6, corresponding to the disappearance of Ferry vortex singularities in presence of the Mach configuration of shock waves. Symbols 1–3 (1, 2 - $M=3$, $\alpha=4$ and 10° ; 3 - $M=6$, $\alpha=4^\circ$) show the values of Mn and ΔK , determined in accordance with mS'^* (α , ϑ , M) and characteristic levels in the distribution of entropy (Fig.10a). There is quite a satisfactory correlation of the criterial values of the parameters in presence and absence of the branch points of shock waves. It should be added that the vortex as a gas-dynamic object of inviscid

origin occurs only when $\delta=0$ and $\vartheta>0$, when flow is separated from the windward outer wing. One should speak about the presence or absence of the Ferry vortex singularity when $\delta>0$.

Conclusion

It was shown that the conical transformation of a V-shaped wing with an opening angle greater than π is an effective means for eliminating the vortex structures on the lee outer wing in the vicinity of the central chord, when the wing is being flown around with a slip. These vortex structures generate critical lines in the conical flow on the surface with intensive spreading flow (critical points of saddle type on a sphere), in the neighborhood of which high heat flows can occur in a real flow. New criteria for the existence of Ferry vortex singularities in absence of the branch points for the internal shock waves, normally incident on the lee outer wing in front of the critical points and realized with $\vartheta>0$ and $\delta>0$, were found.

The work was carried out with a partial financial support of the Russian Foundation for Basic Research (Project No. 18-01-00182) and partially under the state task of the ICAD RAS.

References

1. Zubin M.A., Maksimov F.A., Ostapenko N.A., Criteria of Existence of Nonviscous Vortical Structures in Shock Layers Of Supersonic Conical Gas Flows // *Doklady Physics*. 2014 . Vol.59, №1, pp.49-55.
2. Zubin M.A., Maksimov F.A., Ostapenko N.A., Distinctive features of the shock layer flow structure in conical gas flows // *Fluid Dynamics*, November 2014. Vol.49, №6, pp 804-818.
3. Maksimov F.A., Ostapenko N.A., Zubin M.A. Conical flows near V-shaped Wings with shock waves Attached on leading edges // *Progress in flight physics*. Eds. D. Knight, Ph. Reijasse, and I. Lipatov. EUCASS advances in aerospace sciences book ser. TORUSPRESS-EDPSciences. 2014. Vol. 7, pp.453-474.
4. Maksimov F.A., Ostapenko N.A. V-Shaped Wings with an Opening Angle Exceeding π at Super- and Hypersonic Flow Velocities // *Doklady Physics*. 2016. Vol. 61, №8, pp. 412–417.
5. Zubin M.A., Maximov F.A., Ostapenko N.A. Flow-Around Modes for a Rhomboid Wing with a Stall Vortex in the Shock Layer // *Doklady Physics*. 2017. Vol.62, №12, pp.533-537.
6. Maksimov F.A., Ostapenko N.A., Zubin M.A. V-shaped Wings In Supersonic Flow // *Proc IMechE Part G: Journal of Aerospace Engineering*. 2018.
7. Gonor A.L., Zubin M.A., Ostapenko N.A. Use of Lasers in Experimental Aerodynamics / «Engineering And Automatic Control», Moscow, «Mashinostroyeniye» Publishing House, 1985, pp.5-43.
8. Maksimov F.A., Ostapenko N.A., Zubin M.A. Complex Theoretical and Experimental Investigations of Flow Structure Near V-shaped Wings. *Smart Modeling for Engineering Systems. Proceedings of the Conference 50 Years of the Development of Grid-Characteristic Method*. Springer. 2019, pp.236-245.
9. Zubin M.A., Maksimov F.A., Ostapenko N.A. Control of the Structure of Flow around a Rhomboid Wing in Supersonic Flow // *Doklady Physics*. 2019. Vol.64, №3, pp.125–128.
10. Zubin M.A., Ostapenko N.A. Geometrical Characteristics of Separation of Turbulent Boundary Layer in Case of Interaction with Normal Shock Wave in Conical Flows // *Fluid Dynamics*. 1983. Vol.18, №6, pp.867-875.